Characterization of the Chaotic Magnetic Particle Dynamics

David Laroze[1,2], Jean Bragard[3], Omar J. Suarez[4], and Harald Pleiner[1]

[1]Max Planck Institute for Polymer Research, 55021 Mainz, Germany
[2]Instituto de Alta Investigación, Universidad de Tarapacá, Casilla 7D, Arica, Chile
[3]Departamento de Física y Matemática Aplicada, Universidad de Navarra, 31080 Pamplona, Spain
[4] Departamento de Física, Universidad Técnica Federico Santa Maria, Valparaíso, Chile

In the present work we study the deterministic spin dynamics of an anisotropic magnetic particle in the presence of a time dependent magnetic field using the Landau-Lifshitz equation. In particular, we study the case when the magnetic field is homogeneous with a fixed direction perpendicular to the anisotropy direction and consists of a constant and a time-periodic part. We characterize the dynamical behavior of the system by monitoring the Lyapunov exponents and by bifurcation diagrams. We focus on the dependence of the largest Lyapunov exponent on the magnitude and frequency of the applied magnetic field as well as on the anisotropy parameter of the particle. We find rather complicated landscape of sometimes closely intermingled chaotic and non-chaotic areas in parameter space with rather fuzzy boundaries in-between. For actual experiments that means the system can exhibit multiple transitions between regular and chaotic behavior.

***Index Terms*— Chaotic dynamics, Lyapunov spectrum, magnetization dynamics, time dependent magnetic field.**

I. Introduction

EXPERIMENTAL techniques nowadays have accessed the nanoscale and allow for remarkable developments of new technological applications. Biomedicine or high precision instrumentation are based on nanostructures. A significant application in material science are magnetic particles and clusters for recording media [1]; here, magnetization reversal is a fundamental feature of data storage. The detailed study of the dynamics of magnetic systems is important and will be dealt with here.

In magnetism nonlinear problems have been widely studied, cf. Refs. [2–3]. Models have been used in both, discrete [4–7] and continuous magnetic systems [8–9]. Several experiments of chaotic behaviors in magnetic systems have been reported [10–13]. Typical magnetic samples are yttrium iron garnet spheres [10]. It is worth mentioning that, by ferromagnetic resonance technique, different types of routes of chaos have been found, such as period-doubling cascades, quasi-periodic routes to chaos or intermittent routes to chaos. This implies that there is no universal mechanism leading chaos in these systems, and therefore a theoretical description is highly complicated.

The aim of this paper is to investigate the chaotic dynamics of an anisotropic magnetic nanoparticle under the influence of a time dependent external magnetic field. The latter is assumed to be perpendicular to the anisotropy direction and to consist of a constant and a periodic part. We calculate numerically the Lyapunov exponents and bifurcation diagrams, thus characterizing the dynamical behavior. In particular, the maximum Lyapunov exponent is presented in the form of two-dimensional maps as function of the relevant parameters of the system [14]. In Sec. II, the theoretical model is described, the numerical results are provided and discussed in Sec. III, and finally in Sec. IV a summary is given.

Manuscript received February 17, 2011. Corresponding author: H. Pleiner. (e-mail: pleiner@mpip-mainz.mpg.de).
Digital Object Identifier inserted by IEEE

II. Model

We consider the dynamics of the magnetization $\mathbf{M}$ of a monodomain magnetic particle. The temporal evolution of the system can be modeled by the Landau-Lifshitz equation:

$$\frac{d\mathbf{M}}{dt} = -|\gamma|\mathbf{M}\times\boldsymbol{\Gamma} - \frac{\eta|\gamma|}{M_S}\mathbf{M}\times(\mathbf{M}\times\boldsymbol{\Gamma}), \qquad (1)$$

describing pure rotations, since $|\mathbf{M}|$ is conserved. Here, γ is the gyromagnetic factor, which is associated with the electron spin and whose numerical value is approximately given by $|\gamma| = |\gamma_e|\mu_0 \approx 2.21\times10^5\, m A^{-1} s^{-1}$, and η denotes the dimensionless phenomenological damping coefficient which is a material property with typical values of the order 10^{-4} to 10^{-3} in garnets and 10^{-2} or larger in cobalt or permalloy [3]. For small damping, $\eta^2 \ll 1$, the Landau-Lifshitz equation is equivalent to the Landau-Lifshitz-Gilbert equation [15]. The internal magnetic field, $\boldsymbol{\Gamma}$, acting on the magnetization is given by $\boldsymbol{\Gamma} = \mathbf{H} - \beta(\mathbf{M}\cdot\hat{\mathbf{n}})\hat{\mathbf{n}}$, where $\mathbf{H}$ is the external magnetic field and β measures the anisotropy along the $\hat{\mathbf{n}}$ axis, which we take as the z-axis in the following. This anisotropy is uniaxial and the constant β depends on the specific substance and sample shape [16] and can be positive or negative. The external magnetic field $\mathbf{H}$ is taken along the anisotropy axis. The field strength has a constant and a periodic part $\mathbf{H} = (H_0 + H_1\cos(\omega t))\hat{\mathbf{x}}$ where the amplitudes H_0, H_1 and the frequency ω are constant.

For zero damping $(\eta = 0)$ and without parametric forcing $(H_1 = 0)$ Eq. (1) is conservative. With dissipation and by the periodic injection of energy the magnetic particle is put into an out-of-equilibrium situation. Then, the magnetization of the particle can exhibit a rather complex behavior, e.g., quasi-periodicity, bi-stability and chaos [4]. In the latter reference the existence of chaos due to the external field has been discussed for few parameter values, while in the following we provide a more complete characterization of the chaotic regime, in particular its dependence on the constant field amplitude H_0, the frequency ω, and the anisotropy constant β, thereby revealing a rather complicated structure in parameter space.

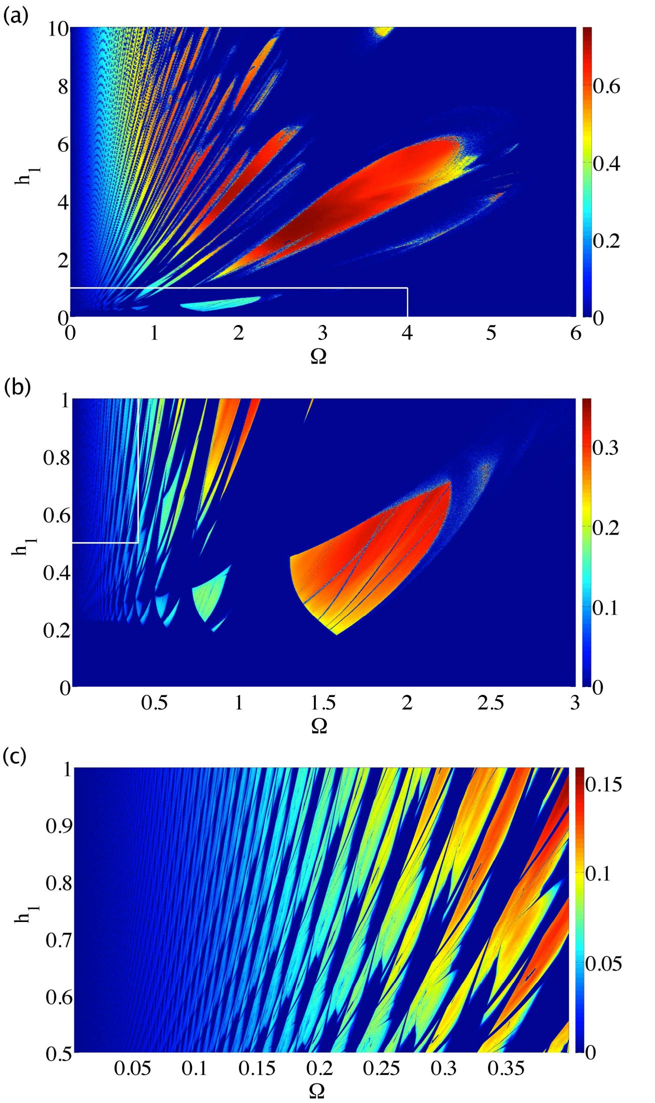

Fig 1: (a) (Color online) The value of the largest positive Lyapunov exponent (LLE) is shown in a color-coded gauge as a function of the amplitude h_1 and the frequency Ω of the driving field for $h_0 = 0.2$, $\beta = 4.8$, and $\eta = 0.02$. Frame (b) depicts the zoomed-in white rectangular area shown in (a) and frame (c) magnifies the white rectangular area of (b). The resolutions are: (a) $\Delta\Omega = 10^{-2}$ and $\Delta h_1 = 5\times10^{-3}$; (b) $\Delta\Omega = 2\times10^{-3}$ and $\Delta h_1 = 5\times10^{-4}$; (c) $\Delta\Omega = 2\times10^{-4}$ and $\Delta h_1 = 2.5\times10^{-4}$.

III. Numerical Results

We analyze the dynamics of Eq. (1) by evaluating the largest Lyapunov exponent (LLE) and by bifurcation diagrams. The exponential divergence of two initially close trajectories, which is characteristic for chaotic dynamics, is quantified by (positive) Lyapunov exponents. From the general theory of dynamical systems it is known those systems with three dynamical degrees of freedom, like the one studied here, cannot have more than one positive Lyapunov exponent [17] and it is, therefore, sufficient to consider the LLE. Exploring the dependence of the LLE on the different parameters of the system, one can identify the areas in parameter space, where the dynamics is chaotic (LLE positive), and those showing regular, periodic or quasiperiodic, dynamics (LLE zero). Following an iterative zoom resolution process explained in Ref. [14], we investigate the dependence of the dynamics on very small variations of the system parameters. This technique is generally utilized for studying dynamical systems that contain chaotic phases with highly complicated and interesting boundary topologies, e.g., curves where networks of stable islands of regular oscillations with ever-increasing periodicities accumulate systematically.

In order to integrate the equations of motion we first scale the magnetization $\mathbf{m} = \mathbf{M}/M_s$ by the saturation magnetization M_s, such that $|\mathbf{m}| = 1$. The time is rendered dimensionless by setting $\tau = t\gamma M_s$ using the appropriate Larmor frequency $1/\gamma M_s$ [3]. Typical experimental values are, e.g. $M_s \approx 1.42\times10^6\,A/m$ for cobalt materials, leading to a time scale $(\tau = 1)$ in the picosecond range, $t_s \approx 3\,ps$. The present technology is able to follow experiments even at the femtosecond scale. Indeed, Beaurepaire et al. [18] were the first to observe the spin dynamics at a time scale below the picosecond scale in nickel [18] and more recently one has observed phenomena at a time scale less than 100 fs [19–20]. By this scaling, the dimensionless field and frequency are $\mathbf{h} = \mathbf{H}/M_s$ and $\Omega = \omega/(\gamma M_s)$, respectively. To avoid numerical artifacts, it is suitable to solve Eq. (1) in the Cartesian representation

$$\frac{dm_x}{d\tau} = h_x\eta\left(m_y^2 + m_z^2\right) + \beta\left(m_y m_z + \eta m_x m_z^2\right) \tag{2}$$

$$\frac{dm_y}{d\tau} = -h_x\left(m_z + \eta m_x m_y\right) + \beta\left(\eta m_y m_z^2 - m_x m_z\right) \tag{3}$$

$$\frac{dm_z}{d\tau} = h_x\left(m_y - \eta m_x m_z\right) - \beta\eta\left(m_x^2 + m_y^2\right)m_z \tag{4}$$

There is a simple homogeneous and stationary solution, $\mathbf{m} = \hat{\mathbf{x}}$, with the magnetization parallel to the magnetic forcing. Driving the system further away from the stationary state, the amplitudes m_y and m_z do not remain small and a rather complicated behavior can occur, including periodic, quasi-periodic and chaotic dynamics.

In order to find the chaotic regimes, we have integrated Eqs. (2)-(4) via a standard fourth order Runge-Kutta integration scheme with a fixed time step $d\tau = 0.01$ guaranteeing a precision of 10^{-8} for the magnetization field. After an initial transient time of $\tau = 1024$ has been discarded, the Lyapunov exponents are calculated during a time span of $\tau = 32768$. The Gram-Schmidt orthogonalization process is performed after every 100th time step. The error er in the evaluation of the Lyapunov exponents has been checked by using $er = \sigma(\lambda_1)/\max(\lambda_1)$, where $\sigma(\lambda_1)$ is the standard deviation of the maximum positive Lyapunov exponent. It is of the order of 1%, which is sufficiently small for the purpose of the present analysis.

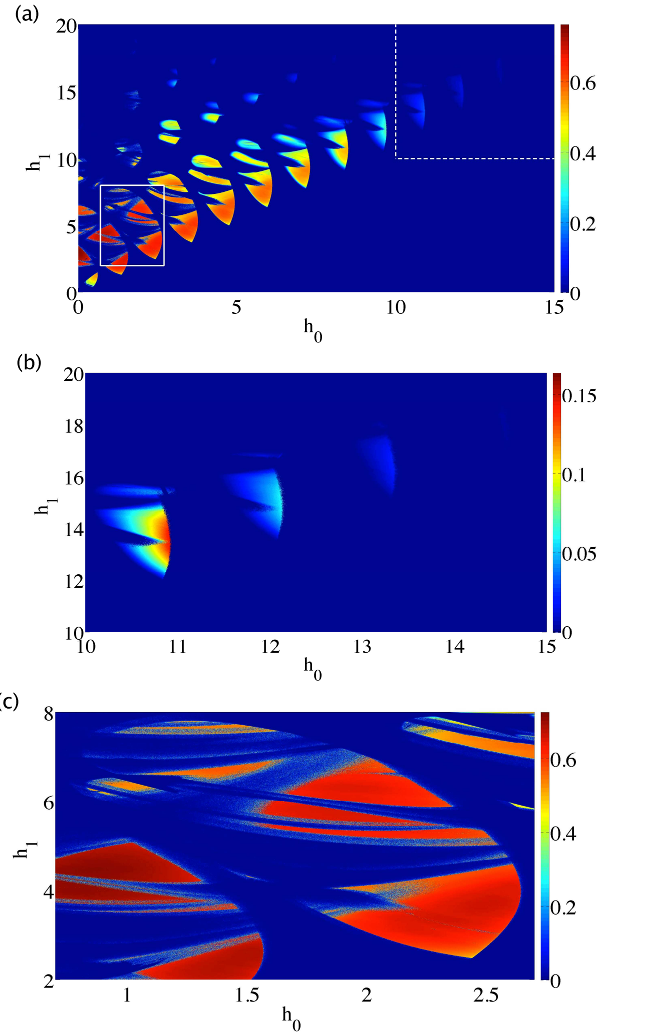

Fig 2: (Color online) The largest Lyapunov exponent (LLE) as a function of h_0 and h_1 at $\Omega = 2.5$, $\beta = 4.8$ and $\eta = 0.02$. Frame (b) represents a zoom of the upper white rectangular area in frame (a), while frame (c) zooms the lower-left white rectangular area. The resolutions are: (a) and (b) $\Delta h_0 = 5\times10^{-3}$ and $\Delta h_1 = 5\times10^{-3}$; (c) $\Delta h_0 = 10^{-3}$ and $\Delta h_1 = 2\times10^{-3}$.

In the following we show how the largest Lyapunov exponent (LLE) depends on two of the relevant parameters keeping the others at fixed values. These 2-dimensional maps are calculated with different, but high resolutions, which are given in the respective figure captions.

First, Fig.(1) (a) shows the color-coded LLE as a function of amplitude h_1 and frequency Ω of the time dependent external field. Frame (b) is a zoom of the area denoted by the white rectangle in frame (a) and frame (c) zooms the white rectangular area of frame (b). There are no chaotic regimes for forcing frequencies well above the natural one, $\Omega \gtrsim 5.5$, indicating that chaos occurs only in the vicinity of the resonance condition. Obviously, chaos requires a sufficiently large value of the field amplitude, $h_x \gtrsim 0.2$, cf. frame(b). Interestingly, inside the larger chaotic areas one can observe small chaos-free areas exhibiting rather complex boundary topologies [14] between chaotic and regular regimes, clearly visible in frame (b). Finally, for small frequencies there is a kind of complex mesh with chaotic and non-chaotic areas interlaced, cf. frame (c). This almost regular pattern continues to exist asymptotically down to zero frequency, where the LLE is vanishing.

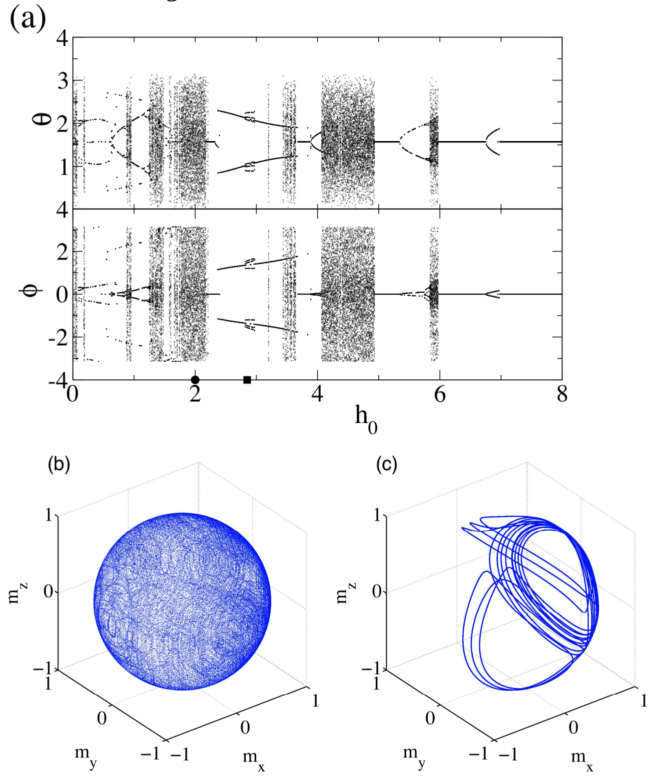

Fig 3: (a) Bifurcation diagrams of θ and ϕ as a function of h_0 at $\Omega = 2.5$, $\beta = 4.8$, $\eta = 0.02$ and $h_1 = 6.5$. Frames (b) and (c) represent the phase portraits for two specific values of h_0: $h_0 = 2$ (b) and $h_0 = 2.85$ (c). They are depicted in the bifurcation diagrams as a dot and a square, respectively.

Secondly, Fig.(2) shows the color-coded LLE as a function of both, the constant and oscillating field amplitude, h_0 and h_1, respectively. Here we fix the frequency at $\Omega = 2.5$, where in Fig.(1) a rich variety of chaotic regions is present. Actually, in this representation the chaotic regions are localized patterns of rather characteristic shapes. They only exist above a line $h_1 \simeq c h_0$ ($c \approx 1$) and rapidly fade away for higher fields as can be seen in frame (b), which is a zoom of the upper white rectangular area in frame (a): The intensity of the LLE decreases and the size of the patterns reduces. The chaotic areas are not compact, but inside they contain zones with regular behavior, cf. frame (c), which zoom the lower-left white rectangular area of frame (a).

Note that, there are other methods of quantifying the non-periodic behavior of a dynamical system [3,4,7,17]. As an example, we calculate bifurcation diagrams using a Poincaré section technique [4] of the magnetization angles, given by $\mathbf{m} = (\cos\phi\sin\theta, \sin\phi\sin\theta, \cos\theta)$. In these diagrams, when there is a continuum of points in the variable the behavior is quasi-periodic or chaotic. The frame (a) of Fig.(3) shows the diagram of θ and ϕ as a function h_0 at time interval multiples of $2\pi/\Omega$, for $h_1 = 6.5$ corresponding to a horizontal line in Fig.(2a). We can observe multiple transitions between regular to non-periodic regimes and for large field the system become regular. The frame (b) and (c) of Fig.(3) shows 3D phase portraits for two fixed values of h_0, extracted form the bifurcation diagrams, in the chaotic and regular regime, respectively.

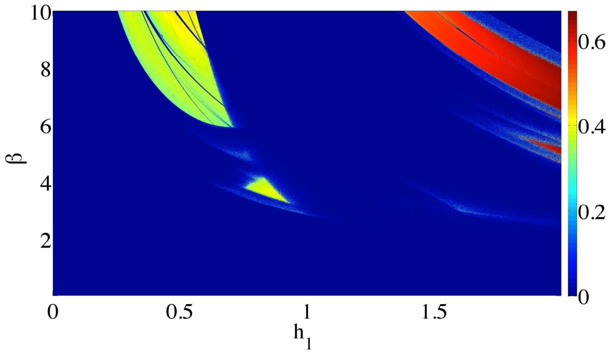

Fig 4: (Color online) The largest Lyapunov exponent (LLE) as a function of h_1 and β at $\Omega = 2.5$, $\beta = 4.8$ and $\eta = 0.02$. The resolutions are: $\Delta h_1 = 10^{-3}$ and $\Delta\beta = 5\times10^{-3}$.

Finally, Fig.(4) shows the color-coded LLE as a function of the forcing field amplitude h_1 and the anisotropy constant β. Again, there is a complicated pattern of chaotic regions that contain smaller regular regions and whose boundaries are rather fuzzy. The minimum field necessary to obtain chaos increases with decreasing anisotropy. However, there are still huge areas of regular dynamics even for intermediate fields irrespective of the anisotropy constant indicating that the anisotropy is a necessary, but by far not a sufficient condition for chaos occurrence.

IV. Summary

The dynamics of the magnetization of an uniaxial anisotropic nanoparticle in the presence of a periodic external magnetic field has been studied using the Landau-Lifshitz equation. We have determined the parameter regions where a positive Lyapunov exponent exists, thereby indicating chaotic dynamics. Extensive numerical calculations have been performed varying simultaneously two parameters in each case. This leads to maps of the chaotic regions as a function of these parameters. For a large range of parameters we find a host of chaotic regimes intricately intermingled with regular ones. Generally, there are no chaotic regions for very small and very large field amplitudes, while even for very small frequencies chaos is possible. A large anisotropy does not necessarily guarantee the existence of chaos.

Acknowledgment

D. L. acknowledges partial financial support from FONDECYT 11080229, Millennium Scientific Initiative, P06-022-F, Basal Program Center for Development of Nanoscience and Nanotechnology (CEDENNA), and Performance Agreement Project UTA/ Mineduc. J.B. acknowledges financial support by Spanish Ministry of Science and Technology under project FIS2008-06335-C02-02.

References

[1] C. Ross, “Patterned magnetic recording media”, *Ann. Rev. Mater. Res.*, vol. 31, pp. 203-235 (2001).

[2] P.E. Wigen (Ed.), *Nonlinear Phenomena and Chaos in Magnetic Materials*, World Scientific, Singapore, 1994.

[3] I.D. Mayergoyz, G. Bertotti, and C. Serpico, *Nonlinear Magnetization Dynamics in Nanosystems*, Elsevier, North Holland, 2009; and references therein.

[4] L.F. Alvarez, O. Pla, and O. Chubykalo, “Quasiperiodicity, bistability, and chaos in the Landau-Lifshitz equation”, *Phys. Rev. B*, vol. 61, pp. 11613-11617 (2000).

[5] D. Laroze and P. Vargas, “Dynamical behavior of two interacting magnetic nanoparticles”, *Phys. B*, vol. 372, pp. 332-336 (2006); D. Laroze and L.M. Perez “Classical spin dynamics of four interacting magnetic particles on a ring”, *Phys. B*, vol. 403, pp. 473-477 (2008); D. Laroze, P. Vargas, C. Cortes, and G. Gutierrez, “Dynamics of two interacting dipoles”, *J. Magn. Magn. Mater.*, vol. 320, pp. 1440-1448 (2008); P. Diaz and D. Laroze, “Configurational temperature for interacting anisotropic magnetic particles”, *Int. J. Bif. Chaos*, vol. 19, pp. 3485-3498 (2009).

[6] D.V. Vagin and P. Polyakov, “Control of chaotic and deterministic magnetization dynamics regimes by means of sample shape varying”, J. *App. Phys.*, vol. 105, 033914 (2009).

[7] R.K. Smith, M. Grabowski, and R.E. Camley, “Period doubling toward chaos in a driven magnetic macrospin”, *J. Magn. Magn. Mater.*, vol. 322, pp. 2127-2134 (2010).

[8] I.V. Barashenkov, M.M. Bogdan, and V.I. Korobov, “Stability Diagram of the Phase-Locked Solitons in the Parametrically Driven, Damped Nonlinear Schrödinger Equation”, *Europhys. Lett.*, vol. 15, pp. 113 (1991).

[9] M.G. Clerc, S. Coulibaly, and D. Laroze, “Localized states beyond the asymptotic parametrically driven amplitude equation”, *Phys. Rev. E*, vol. 77, 056209 (2008); “Nonvariational Ising–Bloch transition in parametrically driven systems”, *Int. J. Bif. Chaos*, vol. 19, pp. 2717-2726 (2009); “Localized states and non-variational Ising–Bloch transition of a parametrically driven easy-plane ferromagnetic wire”, *Phys. D*, vol. 239, pp. 72-86 (2010); “Interaction law of 2D localized precession states”, *Europhys. Lett.*, vol. 90, 38005 (2010).

[10] G. Gibson and C. Jeffries, “Observation of period doubling and chaos in spin-wave instabilities in yttrium iron garnet”, *Phys. Rev. A*, vol. 29, pp. 811–818 (1984)

[11] F. M. de Aguiar, A. Azevedo and S. M. Rezende, “Characterization of strange attractors in spin-wave chaos”, *Phys. Rev. B*, vol. 39, pp. 9448–9452 (1989)

[12] J. Becker, F. Rodelsperger, Th. Weyrauch, H. Benner, W. Just and A. Cenys, “Intermittency in spin-wave instabilities”, *Phys. Rev. E*, vol. 59, pp. 1622-1632 (1999).

[13] J. Cai, Y. Kato, A. Ogawa, Y. Harada, M. Chiba and T. Hirata, “Chaotic dynamics during slow relaxation process in magnon systems”, *J. Phys. Soc. Jap.*, vol. 71, pp. 3087- 3091(2002).

[14] J.A.C. Gallas, “The structure of infinite periodic and chaotic hub cascades in phase diagrams of simple autonomous flows”, *Int. J. Bif. Chaos*, vol. 20, pp. 197-211 (2010); and references therein.

[15] W.M. Saslow, “Landau–Lifshitz or Gilbert damping? That is the question”, *J. Appl. Phys.*, vol. 105, 07D315 (2009).

[16] R.C. O'Handley, *Modern Magnetic Materials: Principles and Applications*, Wiley-Interscience, New York, 1999.

[17] H. Gould and J. Tobochnik, *An Introduction to Computer Simulation Methods: Applications to Physical Systems*, Addison-Wesley, New York, 1996.

[18] E. Beaurepaire, J.C. Merle, A. Daunois, and J.Y. Bigot, “Ultrafast Spin Dynamics in Ferromagnetic Nickel”, *Phys. Rev. Lett.*, vol. 76, pp. 4250-4253 (1996).

[19] B. Koopmans, M. van Kampen, J.T. Kohlhepp, and W.J.M. de Jonge, “Ultrafast Magneto-Optics in Nickel: Magnetism or Optics?”, *Phys. Rev. Lett.*, vol. 85, pp. 844-847(2000).

[20] J. Hohlfeld, E. Matthias, R. Knorren, and K.H. Bennemann, “Nonequilibrium Magnetization Dynamics of Nickel”, *Phys. Rev. Lett.*, vol. 78, pp. 4861-4864 (1997).